Table VI. Low-Energy Conformations of the Linear Pentamer Segment (VPGVG)

RESIDUE	TORSION ANGLES	STRUCTURES A'	B'
Val_1	ϕ	-118	-117
	ψ	131	103
Pro_2	ϕ	-53	-65
	ψ	110	115
Gly_3	ϕ	120	130
	ψ	-57	-70
Val_4	ϕ	-120	-97
	ψ	90	80
Gly_5	ϕ	100	102
	ψ	-175	-166

turn at Pro_2-Gly_3 and the $N_1 \cdots O_4$ hydrogen bond forming a 14-atom ring. Structure B′, on the other hand, while containing the same β turn, shows also a γ turn with an $N_3 \cdots O_5$ hydrogen bond but not the shorter $N_1 \cdots O_4$ distance of a 14-atom ring. These structures are consistent with the NMR data on the linear pentamer.[4,6] Their torsion angles are not very different, and therefore interconversion between the two structures can easily take place. Structure B of *cyclo*-$(VPGVG)_3$ and B′ of the linear pentamer seem to be similar, the essential alteration due to cyclization is seen in the value of the torsion angle ψ_5. Another effect of cyclization may be the inability to form the 14-atom ring as readily in the cyclopentadecapeptide, though this distinction is not particularly evident on comparison of the data on the cyclopentapeptide series with the linear polypentapeptide.[10] In both structures B and C, however, while the $N_1 \cdots O_4$ distance is too long to call a hydrogen bond, the orientation is favorable as seen in the β turn stereo perspectives of Figure 4.

The conformation of *cyclo*-$(VPGVG)_3$ found in the crystal structure[12] is generally similar to structure C derived here. The largest difference is found in the value of ψ_5, which is 122° in the crystal structure. As noted earlier, despite the cyclic nature, *cyclo*-$(VPGVG)_3$ is a rather flexible molecule with the largest flexibility being at the Gly_5 residue. The carbonyls of Val_4 are directed more toward the center of the molecule, in the crystal structure, facilitating interaction with water molecules found inside the cyclic peptide. These solvent interactions and the intermolecular interactions present in the crystal lattice are ignored in the present calculations. In view of these, the degree of agreement between the structure C and the crystal structure is quite satisfying.

The torsion angles of the crystal structure are listed in Table IV. The ϕ angles in the crystal are also indicated in Table II, from which it can be seen that the crystal structure angles all fall well within the allowed ranges obtained from solution NMR coupling constant data.

While the general perspective of structure C approximates that of the crystal, the angles of low-energy structure B may be seen to be quite close to those of the solid-state conformation. Thus, with small changes in torsion angles, one can readily go from structure B to the crystal structure; in this process while the γ turn is ruptured, the size of the central cavity is also increased in order to accommodate the water molecules found in the crystal structure.

Acknowledgment. This work was supported in part by the National Institutes of Health, Grant No. HL-11310 and GM-07195.

The Role of Adsorption in the Initial One-Electron Electrochemical Reduction of Nicotinamide Adenine Dinucleotide (NAD^+)

William T. Bresnahan and Philip J. Elving*[1]

Contribution from the Department of Chemistry, University of Michigan, Ann Arbor, Michigan 48109. *Received June 18, 1980*

Abstract: The title reduction was investigated at pH 9.1 in several base electrolytes of varying surface activity in order to elucidate the role of adsorption of NAD^+, its free radical, and the resulting dimer at the aqueous solution/mercury electrode interface. In the presence of electrolytes of low activity, NAD^+ is adsorbed at potentials positive to its 1-e reduction (ca. −0.9 V vs. SCE); the electrochemically generated dimer, $(NAD)_2$, is adsorbed positive of −1.20 and −1.32 V in 0.06 and 0.4 M KCl solutions, respectively. NAD^+ undergoes both diffusion- and adsorption-controlled reduction; the former predominates on slow time scale experiments and the latter on fast time scales. From low concentration surfactant (0.06 and 0.1 M tetraethylammonium (Tea^+) chloride) solutions, NAD^+ is only adsorbed positive of −0.65 V and an adsorption-controlled prewave appears, indicating that an adsorbed layer of NAD· and/or $(NAD)_2$ is formed on reduction of dissolved NAD^+. From a high concentration (0.4 M) Tea^+ solution, NAD^+ is adsorbed positive of −0.66 V, but the adsorption-controlled prewave is suppressed and the reduction is entirely diffusion controlled. Under diffusion control, the heterogeneous rate constant for the title reduction is ca. 0.1 cm s^{-1} and the rate constant for dimerization of NAD· is ca. 3×10^6 M^{-1} s^{-1}.

β-Nicotinamide adenine dinucleotide (NAD^+; Figure 1) is a high-energy coenzyme of great biochemical importance. In numerous biological hydrogen-transfer reactions, it accepts two electrons and a proton from a substrate (SH_2) in the presence of a suitable enzyme, forming 1,4-dihydronicotinamide adenine dinucleotide (1,4-NADH; Figure 1), the oxidized form of the substrate (S) and a proton.

$$NAD^+ + SH_2 \xrightleftharpoons{\text{enzyme}} \text{1,4-NADH} + S + H^+ \quad (1)$$

The nicotinamide ring is the site of the reversible hydrogen transfer which is stereospecific with respect to both substrate and nicotinamide ring.

Several aspects of the electrochemical behavior of the NAD^+/NADH redox couple have been investigated and reviewed.[2] Cathodic reduction of NAD^+ occurs in two discrete

(1) To whom correspondence should be addressed.

0002-7863/81/1503-2379$01.25/0

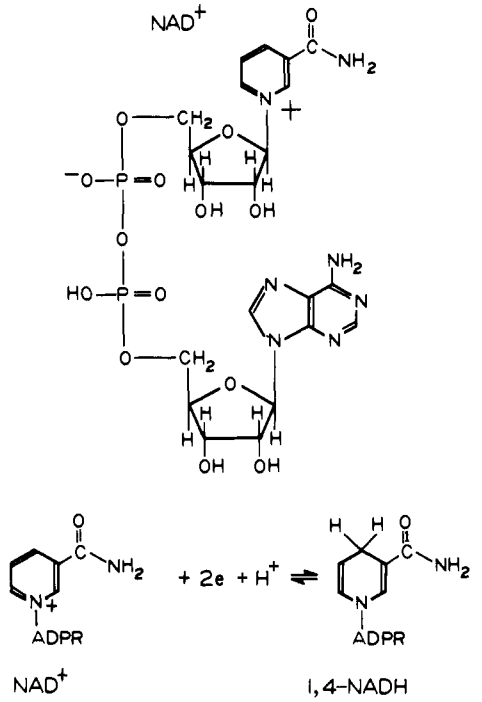

Figure 1. Nicotinamide adenine dinucleotide, NAD^+, in its enzymatically active β form and its biological reduced form, 1,4-NADH. ADPR is adenosine diphosphoribose.

one-electron (1-e) steps; it is reduced (at ca. −1.0 V vs. SCE) to a free radical ($NAD\cdot$) which rapidly dimerizes. The dimer, $(NAD)_2$, is oxidized back to NAD^+ at ca. −0.3 V. At ca. −1.6 V, $NAD\cdot$ is reduced to NADH; both 1,4 and 1,6 isomers are formed. The $NAD\cdot$ reduction is quite complex; e.g., $NAD\cdot$ appears to be intially reduced to an intermediate which rapidly rearranges to the observed product(s) and the primary proton source is the Brønsted acid component of the buffer.[3] Recently, rearrangements subsequent to the 2-e electrochemical reduction of NAD^+ analogues have also been reported.[4]

Among the unanswered questions about the electrochemical behavior of the NAD^+/NADH couple is that of the effect of adsorption on the initial 1-e reduction of NAD^+. Through the addition of varying concentrations of a weak surfactant and the use of a variety of voltammetric techniques, it has been possible in the present study to postulate mechanistic pathways for the initial 1-e reduction, which clarify the roles of the participation of adsorbed and dissolved species.

Experimental Section

Reagents and Solutions. Solutions of NAD^+ (P-L Biochemicals; Chemalog) and NADH (P-L Biochemicals) in distilled water were prepared daily. The background electrolyte consisted of a salt, tetraethylammonium chloride (TeaCl; Eastman) or KCl, and a buffer, Tris (Sigma) or equimolar K_2CO_3 and $KHCO_3$. The total buffer salt concentration was 63 mM; the pH was adjusted to 9.1 with HCl.

Instrumentation and Procedures. A faradaic cage shielded the water-jacketed (25 °C) one-compartment cell[5] with a Luggin capillary and the mercury column. The reference electrode was a saturated calomel electrode against which all potentials are cited. The auxiliary electrode was a Pt wire or gauze. The indicating electrode for polarography was a dropping mercury electrode with a controlled 2.00-s drop time. Purified nitrogen was bubbled through the test solution for at least 20 min prior to and was passed over the solution during electrolysis.

Table I. Direct Current Polarographic Data for the Initial One-Electron Reduction of 0.2 mM NAD^+ in Various Base Electrolyte Solutions at pH 9.1 and 25 °C

base electrolyte				slope,[c]
salt	buffer[a]	I_d[b]	$E_{1/2}$, V	mV
62.5 mM KCl	Tris	1.11	−0.905	72
0.4 M KCl	carbonate	1.21	−0.895	76
62.5 mM TeaCl	Tris	0.99	−0.989	91
0.1 M TeaCl	Tris	1.03	−1.03	97
0.4 M TeaCl	carbonate	1.13	−1.05	60

[a] Concentration = 62.5 mM; pH 9.1. [b] $I_d = \bar{i}/cm^{2/3}t^{1/6}$, $\mu A\ s^{1/2}\ mM^{-1}\ mg^{-2/3}$, where $\bar{i}$ is the mean limiting current. [c] Slope of the log $[i/(i_l - i)]$ vs. E plot.

Electrochemical measurements were generally made with a rapid responsive three-electrode potentiostat,[5] an ancillary function generator, and a suitable recording device. A Princeton Applied Research PAR 174 polarograph was used for pulse polarography. Details for each technique follow.

All polarograms and the voltammograms at a scan rate of less than 0.5 V s^{-1} were recorded with a Houston 2000 or Hewlett-Packard 7005B x-y recorder; rapid phenomena were recorded by a Tektronix 5103N power supply/amplifier oscilloscope base with plug-in modules (5A18N dual trace amplifier; 5B10N time base amplifier; 5A15N amplifier) and C-5A camera. Potentials were monitored with a Hewlett-Packard 3440/3443A digital voltmeter.

DC polarograms obtained with the rapid potentiostat and the PAR 174 were identical within experimental error.

AC polarograms were obtained with a PAR 121 lock-in amplifier/phase detector and the rapid potentiostat with positive feedback. The amplitude of the alternating voltage was 3.54 mV root-mean-square; the frequency is indicated.

A Wavetek 112 function generator and the rapid potentiostat with positive feedback as required were used for cyclic voltammetry. The indicating electrode was a Metrohm 410B hanging mercury drop electrode; the area was determined by weighing 20 drops. Each voltammogram was recorded on a fresh drop. At slow scan rates, peak potentials could generally be estimated at ±3 to 5 mV, depending largely on the peak shape.

Results and Discussion

The initial 1-e reduction of NAD^+ was examined in five different background electrolyte solutions, whose compositions were designed to affect significantly the electrochemical and interfacial behavior of NAD^+ and its reduction products. Each base electrolyte consisted of a salt, either KCl (surface-inactive) or TeaCl (surfactive), and a buffer, either Tris or carbonate (Table I); the salt concentration was varied, but the buffer concentration and pH were held constant at 63 mM and 9.1, respectively. Since the buffer systems did not significantly affect the observed behavior (cf. subsequent discussion), the base electrolytes are generally specified only in terms of their salt component. The NAD^+ concentration was 0.20 mM, unless specified otherwise.

In the Absence of Surfactant. The following results were obtained with solutions which were 63 mM or 0.40 M in KCl and 63 mM in Tris or carbonate buffer, respectively.

(1) Basic Polarographic Pattern. The diffusion current constant,[6] I_d, for the initial 1-e reduction of NAD^+ (Table I; Figure 2) has a temperature coefficient of +1%/°C, as expected for a diffusion-controlled electrode process. The wave slope on logarithmic analysis[7] is somewhat greater than that for a reversible 1-e transfer. Although the reduction is macroscopically reversible,[8]

(2) B. Janik and P. J. Elving, *Chem. Rev.*, **68**, 295 (1968). A. L. Underwood and J. N. Burnett in "Electroanalytical Chemistry", Vol. 6, A. J. Bard, Ed., Marcel Dekker, New York, 1973, p 1. P. J. Elving, C. O. Schmakel, and K. S. V. Santhanam, *CRC Crit. Rev. Anal. Chem.*, 6, 1 (1976). P. J. Elving in "Topics in Bioelectrochemistry and Bioenergetics", G. Milazzo, Ed., Vol. I, Wiley-Interscience, New York 1976, p 278. G. Dryhurst, "Electrochemistry of Biological Molecules", Academic Press, New York, 1977, p 548. R. L. McCreery, *CRC Crit. Rev. Anal. Chem.*, 7, 89 (1978); J. Moiroux and P. J. Elving, *J. Am. Chem. Soc.*, **102**, 6533 (1980).

(3) M. A. Jensen, Ph.D. Thesis, University of Michigan, Ann Arbor, 1977.

(4) Y. Ohnishi, Y. Kikuchi, and M. Kitami, *Tetrahedron Lett.*, **32**, 3005 (1979).

(5) T. E. Cummings, M. A. Jensen, and P. J. Elving, *Electrochim. Acta*, **23**, 1173 (1978).

(6) The diffusion current constant, I_d, equals $\bar{i}_l/cm^{2/3}t^{1/6}$ in $\mu A\ s^{1/2}\ mM^{-1}\ mg^{-2/3}$, where $\bar{i}_l$ is the mean limiting current.

(7) Logarithmic analysis of polarographic or voltammetric waves refers to the plotting of a function of the observed current against the applied potential. From the shape of the resulting line and the numerical slopes of its linear portions, certain deductions can be made concerning the nature of the electrode process which has produced the wave, as subsequently exemplified (cf. A. Weissberger and B. W. Rossiter, Eds., "Techniques of Chemistry", Vol. I, Part IIA, Wiley, New York, 1971).

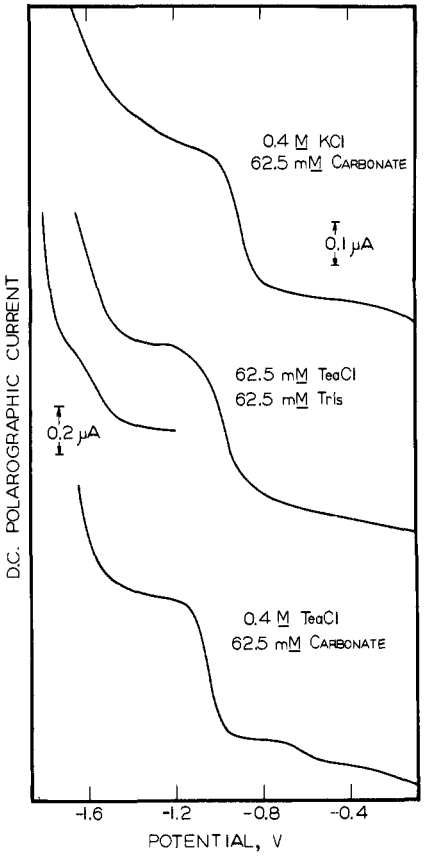

Figure 2. Direct current polarograms of 0.2 mM NAD^+ in base electrolyte solutions of varying surface activity at pH 9.1 and 25 °C. An attenuated curve shows the second one-electron NAD^+ wave in 62.5 mM TeaCl.

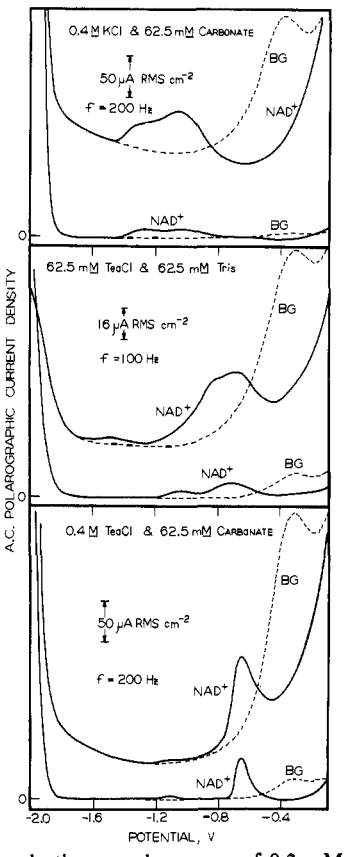

Figure 3. Phase-selective ac polarograms of 0.2 mM NAD^+ in base electrolyte solutions of varying surface activity at pH 9.1 and 25 °C. BG is the background response. The lower set of curves in each case is for the in-phase current component; the upper set is for the quadrature current component. The alternating voltage amplitude is 3.54 mV root-mean-square; the frequency is indicated.

the coupled chemical reaction (dimerization of the free radical) and possible adsorption of NAD^+, $NAD\cdot$, and/or $(NAD)_2$ will affect the kinetics and energetics of the process and, consequently, the transition state involved in the rate-determining step, which effects will be mirrored in the wave slope and $E_{1/2}$. Thus, the $E_{1/2}$ of −0.9 V indicates that adsorption accompanies the reduction; a potential of −1.0 V is observed when a surface-active ion, e.g., Tea^+, is also present (ref 8 and the following sections). Adsorption of NAD^+ slightly decreases the charging current at potentials more positive than the potential of zero charge (pzc) and increases the charging current at more negative potentials. In 63 mM KCl, only the foot of the second 1-e wave may be seen prior to background discharge which starts at ca. −1.6 V. In 0.4 M KCl, the second wave is seen, and $E_{1/2}$ for the first wave is 20 mV more positive and I_d is 9% larger than in 63 mM KCl.

(2) Adsorption Characteristics. The essential features (Figure 3) are the same in 63 mM and 0.4 M KCl.

AC polarographic in-phase currents in the presence and absence of NAD^+ are equal except near −1.0 V, where NAD^+ reduction occurs, and near −0.3 V, where an interface change (involving chloride ion) occurs in the absence of NAD^+ and a small peak appears.

The quadrature current in the presence of NAD^+ is depressed below that for base electrolyte alone at potentials positive of the initial 1-e reduction, indicating that NAD^+ is adsorbed in the region positive of the tensammetric peak at −1.08 V. The quadrature current negative of −1.20 V in 63 mM KCl and −1.32 V in 0.4 M KCl is unchanged by the presence of NAD^+, indicating preferential adsorption of base electrolyte. $(NAD)_2$ is adsorbed positive of its tensammetric peak at −1.20 or −1.32 V; this peak has been attributed to $(NAD)_2$ since it alone appears in the presence of $(NAD)_2$ and the absence of NAD^+.[8] From the higher ionic strength solution, $(NAD)_2$ is more strongly adsorbed and is adsorbed over a wider potential region, resulting in the shift of the tensammetric wave to more negative potential.

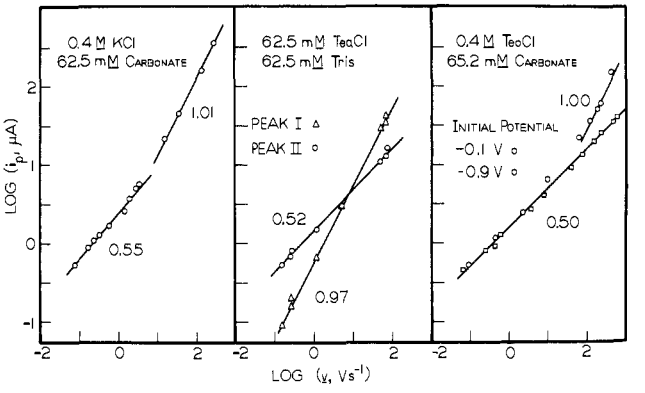

Figure 4. Variation of the cyclic voltammetric peak current (i_p) with scan rate (v) for 0.2 mM NAD^+ in base electrolyte solutions of varying surface acticity at pH 9.1 and 25 °C. Electrode area = 0.0184 cm^2. Slopes of the lines are given.

(3) Controlling Processes. The cyclic voltammetric (CV) behavior for the initial 1-e reduction of NAD^+ (Figure 4; Table II) reveals the presence of both diffusion- and adsorption-controlled processes.

For scan rate, v, less than 1.5 V s^{-1}, the CV current function, $i_p/Acv^{1/2}$,[9] is nearly constant (slope is ca. 0.5), indicating a predominantly diffusion-controlled reduction. The function should decrease slightly (no more than 10%) with increasing v for a purely diffusion-controlled electron transfer with consecutive irreversible

(8) C. O. Schmakel, K. S. V. Santhanam, and P. J. Elving, *J. Am. Chem. Soc.*, 97, 5083 (1975).

(9) Units for i_p/Acv are μA s cm^{-2} mM^{-1} V^{-1}; for $i_p/Acv^{1/2}$, units are μA $s^{1/2}$ cm^{-2} mM^{-1} $V^{-1/2}$.

Table II. Effect of Scan Rate (v) on the Cyclic Voltammetric Behavior of NAD^+ at pH 9.1 and 25 °C[a]

v, V s^{-1}	$-E_p$, V	i_p/Acv	$i_p/Acv^{1/2}$	i_p/Acv
0.798	0.945	1730	490[b]	
0.182	0.945	1270	540	
0.241	0.950	1160	570	
0.339	0.960	980	570	
0.594	0.960	740	570	
1.50	0.97	450	550	
1.96	0.97	500	700	110[c]
2.98	0.99	440	750	120
3.44	0.99	440	810	140
15.5	1.00	360	1400	220
35.6	1.01	330	2000	240
144	1.08	290	3500	240
290	1.08	320	5500	290

[a] Background is 0.4 M in KCl and 62.5 mM in carbonate; NAD^+ concentration (c) = 0.209 mM; electrode area (A) = 0.0184 cm^2. Current units are given in reference 9. [b] For $v \leq 1.50$ V s^{-1}, mean = 550 and range = 490–570. [c] Values of i_p have been corrected for the contribution to the current by the diffusion-controlled process. Mean = 250 for $v \geq 15.5$ V s^{-1}.

dimerization.[10] An appreciable decrease is not observed; this may be due to adsorption of NAD^+ or experimental error.

For $v > 15$ V s^{-1}, i_p/Acv is nearly constant (slope is ca. 1.0), indicating a predominantly adsorption-controlled reduction. For diffusion-control, $i_p/Acv^{1/2}$ (calculated from data for $v \leq 1.5$ V s^{-1}) is 550; this value can be used to correct i_p at high v for the contribution due to diffusion. For the corrected peak currents, i_p/Acv is nearly constant at 250 for $v > 15.5$ V s^{-1}. Thus, at high v, the peaks consist of adsorption- and diffusion-controlled components which appear at the same potential; at low v, the currents are primarily diffusion controlled.

Since no prepeak or postpeak is observed in 0.4 M KCl, under these conditions, the strengths of adsorption of NAD^+ and NAD· are nearly equal. The peak shifts to more negative potential with increasing v, as expected for a chemical reaction following electron transfer. Similar peak shifts are observed in TeaCl solutions.

In the Presence of Low Surfactant Concentrations. Consideration of the behavior of NAD^+ in presence of a weak surfactant (Tea^+) is facilitated by discussing separately the results obtained at low and high Tea^+ concentrations. The following results were obtained with solutions which were 63 or 100 mM in TeaCl and 63 mM in Tris buffer.

(1) Basic Polarographic Pattern. The initial 1-e reduction wave of NAD^+ is considerably more drawn out in the low concentration TeaCl than in KCl or high concentration TeaCl (Figure 2; Table I); $E_{1/2}$ in TeaCl is shifted negatively with respect to the KCl solutions and is about 40 mV more negative in 100 mM TeaCl than in 63 mM TeaCl, although the slopes are approximately equal and considerably larger than in KCl and high TeaCl concentration. Although it is not apparent from the dc polarographic wave, NAD^+ is reduced via two distinct processes at the low TeaCl concentrations. On ac polarography, CV, and pulse polarography, an adsorption-controlled process appears as a preprocess to the diffusion-controlled process. This unresolved prewave accounts for the drawn-out nature of the dc wave which is reflected in its slope of 90+ mV.

(2) Adsorption Characteristics. The ac polarograms for NAD^+ are quite different from those seen in KCl or high TeaCl concentration (Figures 3 and 5).

Two in-phase current peaks appear at −0.74 V and −1.04 V. The latter is a component of the faradaic current for the 1-e NAD^+ reduction. The former is a component of the NAD^+ tensammetric peak. At 63 mM TeaCl, no activity appears negative of −1.2 V; i.e., the reduction of NAD· is not observed at the concentration and sensitivity involved.

The quadrature current for 63 mM TeaCl solutions is depressed by the presence of NAD^+ below that for base electrolyte alone,

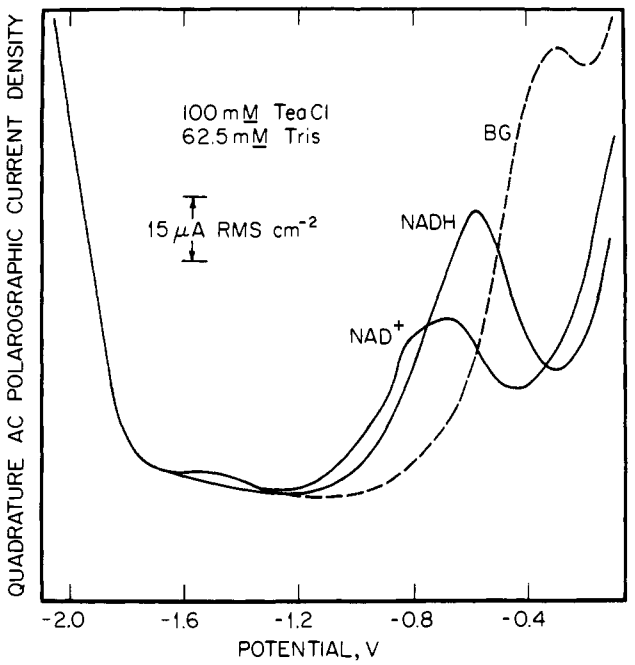

Figure 5. Alternating current polarographic quadrature current polarograms for 0.2 mM NAD^+, 0.2 mM NADH, and background base electrolyte (BG) (0.1 M TeaCl and 62.5 mM Tris) at pH 9.1 and 25 °C. The alternating voltage amplitude is 3.54 mV root-mean-square; the frequency is 100 Hz.

positive of −0.61 V (−0.85 V in KCl); NAD^+ is adsorbed in this region. With NAD^+ present, three poorly resolved quadrature peaks appear between −0.5 and −1.2 V. The first and second correspond to the in-phase peak at −0.74 V; that at −0.72 V is the NAD^+ tensammetric peak; that at −0.84 V is due to the pseudocapacitance associated with adsorption of the reduction product, i.e., NAD· and/or $(NAD)_2$ (the nature of this peak is subsequently discussed). The third, which is just a shoulder at −1.08 V, corresponds to the in-phase peak at −1.04 V and is a component of the faradaic current for the 1-e NAD^+ reduction. At 100 mM TeaCl, the quadrature current is greater in the region from −0.5 to −1.2 V and a fourth, more negative, peak appears (cf. following discussion).

NADH was chosen to model the adsorption of NAD^+ because of the obvious structural similarities (Figure 1) and its simpler polarographic pattern due to the absence of faradaic components; e.g., a 0.20 mM NADH solution exhibited no dc polarographic waves in the potential region available on mercury. The difference in charge on the nicotinamide ring in the two compounds should induce only a small difference in adsorption which occurs primarily through the adenine moiety.

For both NAD^+ and NADH, the quadrature current is depressed below that of background in the region positive of −0.5 V, where they are adsorbed. NAD^+ exhibits four quadrature peaks; NADH exhibits only one peak (Figure 5). For NAD^+, the peaks arise from (a) the tensammetric effect at −0.67 V, (b) the pseudocapacity at −0.84 V arising from reduction product adsorption, (c) the faradaic component for NAD^+ reduction which appears as a shoulder at −1.04 V, and (d) the faradaic component for NAD· reduction at −1.5 V. The lone NADH tensammetric peak at −0.58 V is 90 mV positive of the NAD^+ tensammetric peak; the shift probably reflects the difference in net charge on the two species at pH 9.1 (2- on NADH; 1- on NAD^+). Due to coulombic attraction to the electrode, the more negative species (NADH) should desorb at a less negative potential.

If the peaks due to faradaic processes are ignored, the NAD^+ quadrature polarogram resembles quite closely that of NADH, indicating very similar adsorption of the two compounds over the available potential range.

(3) Controlling Processes. A slow-scan cyclic voltammogram (Figure 6) illustrates the processes operative at low TeaCl concentrations. NAD^+ is reduced in 1-e processes at −0.86 and −1.06

(10) M. L. Olmstead, R. G. Hamilton, and R. S. Nicholson, *Anal. Chem.*, **41**, 260 (1969).

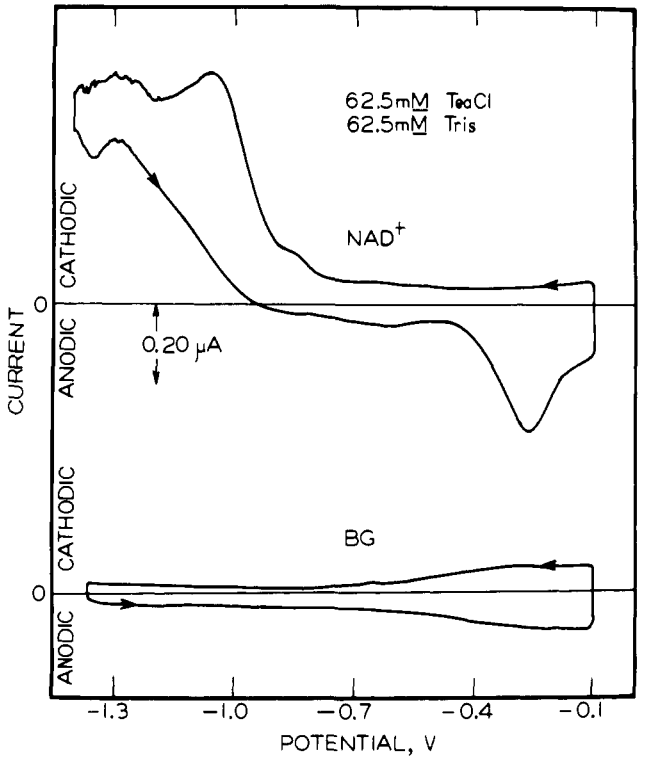

Figure 6. Cyclic voltammogram of 0.20 mM NAD^+ at pH 9.1 and 25 °C. Background electrolyte (BG) is 62.5 mM in TeaCl and 62.5 mM in Tris. Scan initiated at −0.10 V; arrows show the scan direction; scan rate = 0.10 V s^{-1}; electrode area = 0.0184 cm^2.

V; the noisy region near −1.3 V in both scan directions probably results from stripping of adsorbed $(NAD)_2$. Since the dimerization is very rapid, no oxidation is observed on the positive scan until that of $(NAD)_2$ to NAD^+ at −0.27 V; the latter peak shifts positively with increasing v and is not resolved from the oxidation of Hg in the presence of chloride at $v > 10$ V s^{-1}. In the absence of NAD^+ (Figure 6), only broad capacitive peaks near −0.3 V appear; similar but smaller peaks occur near −0.65 V with NAD^+ present.

Voltammograms obtained in KCl and high TeaCl concentration have the same essential features as shown in Figure 6, except that the prepeak is seen at the low TeaCl concentration. An anodic peak due to oxidation of NAD· to NAD^+ is seen only at very high scan rates.

The i_p/Acv and $i_p/Acv^{1/2}$ ratios for NAD^+ initial 1-e reduction peaks I and II, respectively, are constant as a function of v (Table III; Figure 4). Up to v of 69 V s^{-1}, peak II meets the criterion that, for a reversible 1-e reduction followed by dimerization, $i_p/Acv^{1/2}$ should vary less than 10%;[10] peak I does not for any range of v. Conversely, the constancy of i_p/Acv for peak I indicates that it is due to reduction of NAD^+ to an adsorbed product, NAD· and/or $(NAD)_2$; the adsorption, as expected, is less at the high TeaCl concentration; i.e., i_p/Acv is 170 at 63 mM TeaCl and 84 at 100 mM. The variations in the current functions are due at least in part to increased uncertainty in their measurements at high v resulting from overlap of the two peaks. The negative shift of E_p for both peaks with increasing v is expected when an irreversible chemical reaction (dimerization) follows electron transfer whether the product is adsorbed or not. The diffusion-controlled process becomes buried under the adsorption-controlled peak at very high v.

At low v, the prepeak (peak I) occurs at the same potential (−0.87 V) as the second quadrature peak (Figure 3); this coincidence substantiates assignment of the peak as due to pseudocapacitance associated with adsorption of NAD· and/or $(NAD)_2$.

On normal pulse polarography (NPP) at 18 and 25 °C, NAD^+ exhibits a prewave at −0.87 V, a well-formed sigmoidal wave at −1.03 V, and a third wave just resolved from background discharge at −1.62 V (Figure 7). The prewave corresponds to reduction

Table III. Effect of Scan Rate (v) on the Cyclic Voltammetric Behavior of NAD^+ at pH 9.1 and 25 °C

	peak I[f]		peak II[f]	
v, V s^{-1}	E_p, V	i_p/Acv	E_p, V	$i_p/Acv^{1/2}$
Background: 62.5 mM TeaCl and 62.5 mM Tris				
0.099[a]	−0.86	200[b]	−1.06	410[c]
0.155	−0.88	170	−1.07	380
0.255	−0.89	180	−1.07	400
0.330	−0.90	170	−1.07	400
1.20	−0.91	150	−1.09	390
5.08	−0.96	170	−1.11	380
9.50[a]	−0.94	190	−1.09	440
5.04	−0.98	160	−1.10	440
68.0	−1.01	140	−1.11	450
76.0	−1.01	160	−1.12	520
95.0[a]	−1.02	150	−1.10	500
250[a]	−1.05	170	[d]	
Background: 0.10 M TeaCl and 62.5 mM Tris				
0.170[e]	−0.87	89	−1.07	380
0.255	−0.88	85	−1.08	370
0.340	−0.90	80	−1.09	370
3.46	−0.95	94	−1.09	380
20.9	−0.99	72	−1.12	380
33.0	−0.99	88	−1.12	410
210	−1.05	77	[d]	

[a] Electrode area (A) = 0.0244 cm^2 and NAD^+ concentration (c) = 0.200 mM; otherwise, A = 0.0182 cm^2 and c = 0.0193 mM. [b] Mean is 170 for a range of 140–200. [c] Mean is 410 for $v \leq 68$ V s^{-1} with a range 380–450. [d] Peak II is buried under peak I at this scan rate. [e] Electrode area (A) = 0.0183 cm^2 and NAD^+ concentration (c) = 0.202 mM. [f] Current units are given in reference 9.

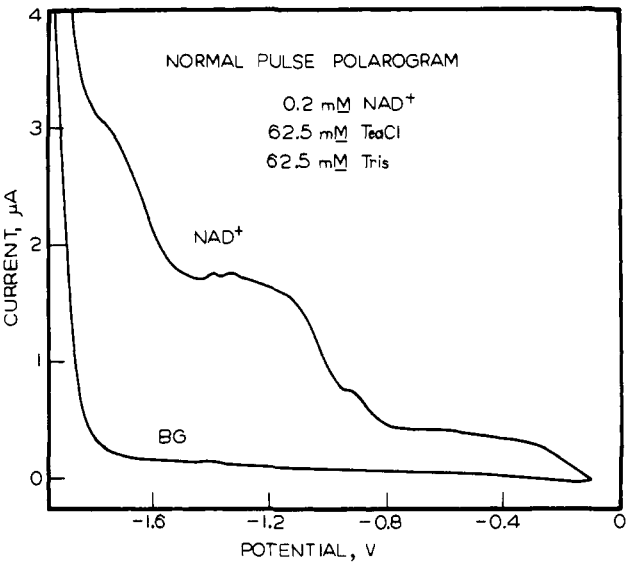

Figure 7. Normal pulse polarogram of 0.20 mM NAD^+ at pH 9.1 and 25 °C. Background electrolyte (BG) is 62.5 mM in TeaCl and 62.5 mM in Tris. Initial potential = −0.10 V; delay time = ca. 48 ms.

of NAD^+ to adsorbed NAD·; the second and third waves correspond to diffusion-controlled reductions of NAD^+ and NAD·, respectively.

In the Presence of High Surfactant Concentration. The following results were obtained with a solution which was 0.40 M in TeaCl and 63 mM in carbonate.

(1) Basic Polarographic Pattern. Logarithmic analyses for the initial NAD^+ reduction wave (Table I; Figure 2) are given in Figure 8 for several NAD^+ concentrations. The plots should have limiting slopes of 39 mV at the foot of the wave and 120 mV in the plateau region;[11-13] the experimental data (Figure 8) agree

(11) R. Bonnaterre and G. Cauquis, *J. Electroanal. Chem.*, **32**, 199 (1971).

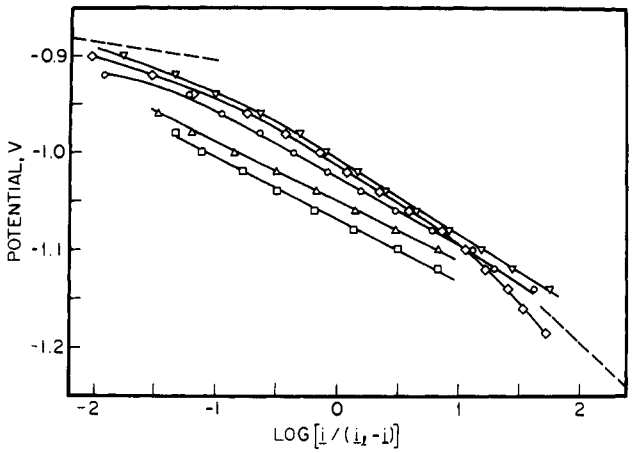

Figure 8. Logarithmic analyses of the initial one-electron reduction wave of NAD^+ at pH 9.1 and 25 °C. Millimolar concentration of NAD^+: rectangles, 0.0493; triangles, 0.204; circles, 0.403; diamonds, 0.745; inverted triangles, 1.12. Background is 0.4 M in TeaCl and 62.5 mM in carbonate. Dashed lines are the theoretical limiting slopes of 39 and 120 mV.

Table IV. Effect of Scan Rate (v) and Initial Potential (E_i) on the Cyclic Voltammetric Behavior of NAD^+ at pH 9.1 and 25 °C[a]

v, V s^{-1}	$-E_p$, V	i_p/Acv	$i_p/Acv^{1/2}$	i_p/Acv
		$E_i = -0.100$ V		
0.094	1.10	1480	450	110[b]
0.448	1.12	700	470	73
2.34	1.13	280	430	4
9.6	1.14	180	550	42
25.6	1.14	120	630	42
60	1.15	100	760	43
122	1.17	79	870	40
184	1.17	74	1000	43
248	1.17	64	1020	38
432	1.17	54	1120	33
		$E_i = -0.900$ V		
0.048	1.11		460[c]	
0.247	1.11		420	
0.417	1.11		460	
0.590	1.12		460	
3.54	1.13		380	
7.92	1.14		380	
40	1.16		390	
78.5	1.16		410	
154	1.17		410	
231	1.18		440	
493	1.19		430	
616	1.21		420	

[a] Background is 0.4 M in TeaCl and 62.5 mM in carbonate; NAD^+ concentration (c) = 0.204 mM; electrode area (A) = 0.0184 cm^2. Current units are given in reference 9. [b] Values of i_p have been corrected for the contribution to the current by the diffusion-controlled process. Mean is 40 for v from 9.6 to 432 V s^{-1}. [c] Mean is 440 for a range of 380–460.

reasonably well, especially at higher concentrations where current measurements in the wave foot and plateau regions are more accurate. The theoretical dependence of $E_{1/2}$ on log of concentration is 19.7 mV/decade; the data (Figure 9) agree qualitatively but the observed slope of 48 mV is perplexing. The $E_{1/2}$ are also more positive than expected, on the basis of the dimerization rate calculated from fast scan CV.[13] These anomalies may be due to some effect of adsorption of NAD^+ or its reduction products, which is not completely suppressed by the adsorption of Tea^+ and which becomes more apparent with increasing NAD^+ concentration or in the absence of Tea^+ (cf. discussion of $E_{1/2}$ in KCl solution).

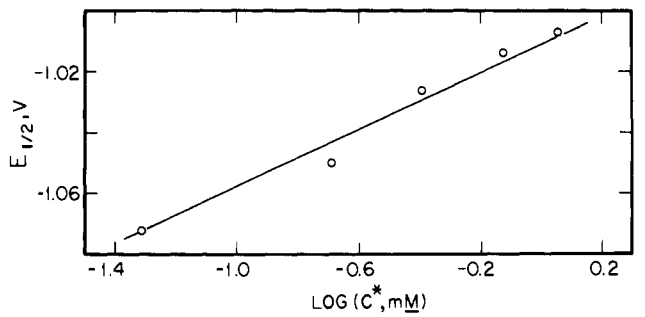

Figure 9. Dependence of half-wave potential, $E_{1/2}$, upon bulk concentration, C^*, of NAD^+ at pH 9.1 and 25 °C. Base electrolyte is 0.4 M TeaCl and 62.5 mM in carbonate. Slope of the dependence is 48 mV/decade.

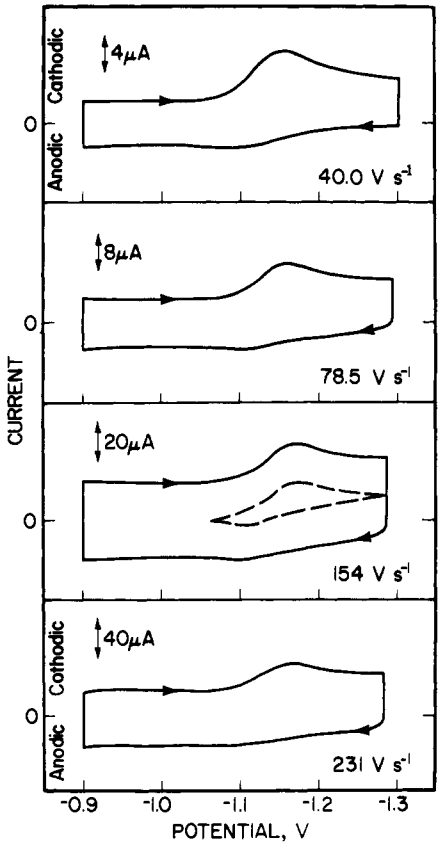

Figure 10. Fast-scan cyclic voltammograms for 0.204 mM NAD^+. Background is 0.4 M in TeaCl and 62.5 mM in carbonate at pH 9.1 and 25 °C. Scans are initiated at −0.90 V; arrows show the scan direction; scan rates are given; electrode area = 0.0184 cm^2. Positive feedback was used for iR compensation. The dashed line in the third panel shows the faradaic current after subtraction of the charging current. The latter is measured at potentials at which no faradaic activity occurs and is assumed not to vary with potential; this assumption introduces up to 10% error in peak current measurement and up to 10-mV error in peak potential measurement. Within such limits, the separation of the anodic and cathodic peaks is 60 ± 20 mV.

The small wave at −0.66 V is capacitive in nature[14] and occurs at the same potential as the ac tensammetric peak, as subsequently discussed. A capacitive peak is also seen on CV.

(2) Adsorption Characteristics. Positive of the tensammetric peak at −0.66 V, NAD^+ is adsorbed (Figure 3). The quadrature components differ significantly from those in low TeaCl concentrations. In 0.4 M TeaCl, the NAD^+ tensammetric peak at −0.66 V is at nearly the same potential as at low TeaCl concentrations, but the adsorption of NAD· and/or $(NAD)_2$ is blocked;

(12) J. Jacq, *Electrochim. Acta*, **12**, 1345 (1967).
(13) Z. Samec, W. T. Bresnahan, and P. J. Elving, work in progress.
(14) C. O. Schmakel, M. A. Jensen, and P. J. Elving, *Bioelectrochem. Bioenerg.*, **5**, 625 (1978).

i.e., the pseudocapactive peak at −0.87 V does not appear and the tensammetric wave is quite sharp. Furthermore, a quadrature current peak does not appear for the NAD· reduction.

(3) Controlling Processes. The CV behavior of NAD^+ is grossly dependent on E_i and the time scale (scan rate) of the experiment (Figures 4 and 10; Table IV).

When E_i = −0.10 V, where NAD^+ is adsorbed, $i_p/Acv^{1/2}$ for the initial 1-e reduction is constant (slope is ca. 0.5) up to v of 10 V s^{-1} and i_p/Acv is nearly constant (slope is ca. 1.0) at $v >$ 100 V s^{-1}; i.e., the current is diffusion-controlled at low v and adsorption controlled at high v; at intermediate v, the magnitudes of the currents controlled by adsorption and diffusion are nearly equal. A similar pattern is seen in 0.4 M KCl (Table II; Figure 4).

When E_i = −0.90 V, where NAD^+ is not adsorbed, $i_p/Acv^{1/2}$ is nearly constant at 420, indicating diffusion control. Correction for the contribution due to diffusion of the CV peak currents for E_i = −0.10 V results in i_p/Acv being nearly constant at 40 for v between 9.6 and 432 V s^{-1} (Table IV). Thus, the peaks at high v, when E_i = −0.10 V, arise from two processes whose peak currents occur at nearly the same potential.

When the NAD^+ concentration exceeds 0.2 mM, the CV currents are still diffusion controlled at low v and adsorption controlled at high v, but the change from diffusion to adsorption control is less obvious than at 0.2 mM, which is probably why the present behavior has not been reported previously.

(4) Dimerization Rate Constant. When transport of the reactants to the electrode is diffusion controlled (i.e., reactant and product are not adsorbed and charge transfer is reversible), the rate constant, k_d, for dimerization consecutive to 1-e transfer can be evaluated from a working curve of the anodic to cathodic peak current ratio, i_{pa}/i_{pc}, as a function of log $(k_d c\tau)$, where c is the bulk concentration of the initial reactant and τ is the time needed to scan from the formal potential to the switching potential.[10] Thus, for NAD^+, the method is usable in 0.4 M TeaCl only with an E_i at which NAD^+ is not adsorbed since high v and low concentrations are necessary in measuring k_d. The method is not valid in the low concentration TeaCl solutions and is only valid in KCl solutions at v where i_p is diffusion controlled.

For E_i = −0.90 V, v between 36 and 493 V s^{-1}, and c of 0.20 and 0.40 mM, k_d for NAD· is found to be $(2.7 \pm 2.3) \times 10^6$ M^{-1} s^{-1} (mean and standard deviation for 8 measurements) in 0.4 M TeaCl and 63 mM carbonate (pH 9.1) at 25 °C.

To demonstrate the error in k_d introduced by initiating the fast scan at a potential where NAD^+ is adsorbed, e.g., −0.10 V, we calculated a k_d of 9×10^6 M^{-1} s^{-1} for these conditions. Although there is considerable uncertainty in the present results due primarily to the difficulty in measuring i_{pa} at high v, the increase in apparent k_d, due to the increased i_{pa} resulting from reduction of adsorbed NAD^+, appears to be real.

On the basis of a cyclic chronopotentiometrically estimated free radical half-life of less than 1 ms at pH 8, k_d was considered to exceed 10^6 M^{-1} s^{-1}.[15] Although it was noted that adsorption vitiated the assumptions for evaluation of k_d from E_p shift, a k_d of 8.49×10^6 at pH 7 was reported.[16] On the basis of CV peak current ratio method,[10] values were obtained of $(2.2 \pm 0.6) \times 10^6$ M^{-1} s^{-1} in 0.5 M ionic strength acetate buffer at pH 5.0 and $(2.4 \pm 2.1) \times 10^6$ M^{-1} s^{-1} in 0.5 M ionic strength carbonate buffer (0.4 M in KCl) at pH 9.0; 8 these results, which are viable since diffusion-controlled currents were used for the calculations, are in excellent agreement with those obtained in the present study even though different base electrolytes were used.

Even at high v, the CV peaks shift slightly negatively on increase in v, indicating that the reduction is not completely reversible. $E_c°$, taken as the mean of E_{pc} and E_{pa}, ranges from −1.130 to −1.150 V. Fast scan CV gave an $E_c°$ of −1.155 V in 0.4 M TeaCl and 0.1 M carbonate (pH 9.1). Although the current ratio method for evaluation of k_d requires a reversible reaction,[10] the slight irreversiblity (quasi-reversibility) of the NAD^+ reduction should only slightly affect the present evaluation of k_d.

(5) Heterogeneous Charge-Transfer Rate Constant. Based on i–E curve parameters obtained by numerical solution of an integral equation describing the CV behavior of a redox couple, Marecĕk and Honz[17] have tabulated data from which the electrochemical heterogeneous rate constant at the formal potential, $k_s°$, for a simple electrode reaction

$$O + ne^- \rightleftarrows R \qquad (2)$$

can be calculated. Although the 1-e reduction of NAD^+ is followed by dimerization, the reduction approaches a simple reaction at high v where i_{pa}/i_{pc} approaches unity. On the basis of $E_c°$ = −1.123 V[13] and the shifts in E_{pc} and in potential where the current equals 0.5 i_{pc} as a function of v (Figure 10), $k_s°$ was found to be ca. 0.1 cm s^{-1}. Since it was not possible to check this value by determining $k_s°$ from the E_{pa} shift, because the latter could not be measured with the necessary certainty, the value of 0.1 cm s^{-1} is approximate.

Mechanistic Pathways

Adsorption and Conformation Factors. The adenine moiety of NAD^+ has an important effect on the electrochemical behavior of the coenzyme;[14] e.g., it is largely responsible for the adsorption of NAD^+ in the potential region near and positive of the electrocapillary maximum. Our working model for the orientation of adsorbed NAD^+ at the electrode/solution interface consists of the adenine ring flat on the surface with the coenzyme in a *folded* conformation, i.e., with the nicotinamide ring parallel and close to the adenine ring. This folded conformation at the interface evokes the concept of electron transfer from the electrode through the adenine ring to the nicotinamide moiety.[18]

The difference of 0.1 V in $E_{1/2}$ for the initial 1-e NAD^+ reduction between solutions of surface-inactive and surfactive electrolytes is due to a combination of factors, including adsorption of NAD^+ and/or its reduction products, e.g., presence of an unresolved prewave affects $E_{1/2}$, and the rate of NAD· dimerization; e.g., $E_{1/2}$ is a function of k_d and concentration; k_d may be strongly influenced by adsorption of NAD^+ and/or its reduction products.

Adsorption may influence the reversibility of the electron transfer as reflected in the wave slope; presence of an unresolved prewave will increase the slope. At higher NAD^+ concentrations in 0.4 M TeaCl, where the reduction is most reversible and diffusion controlled, the log plot shows the expected[11] nonlinearity with limiting slopes of 39 and 120 mV in the wave foot and plateau regions, respectively.

The increase in I_d with increasing ionic strength in both surfactive and nonsurfactive electrolyte solutions may largely reflect the conformation of the dinucleotide in solution. At higher ionic strength, NAD^+ probably exists in a more compact conformation with the greater intramolecular attraction between the nicotinamide and adenine rings, resulting in a smaller effective cross-sectional area with a consequently lower barrier to diffusion. The fact that I_d is slightly lower in TeaCl than in KCl solutions of the same ionic strength suggests that Tea^+-adsorbed layer(s) are a greater barrier to diffusion than K^+.

Mechanistic Pathways. From the variation in voltammetric and polarographic patterns of NAD^+ with nature of the base electrolyte solution, mechanistic pathways for the initial 1-e reduction of NAD^+ can be deduced, especially in regard to the role of adsorption (Figure 11).

Although Tris was used to buffer the low concentration base electrolyte solutions and carbonate the high concentration solutions, differences in the mechanistic pathways in these solutions are largely if not entirely due to the salt nature and concentration which govern the composition of the solution/electrode interface. The nature of the buffer is not expected to affect the pathways

(15) A. M. Wilson and D. G. Epple, *Biochemistry*, **5**, 3170 (1966).
(16) A. J. Cunningham and A. L. Underwood, *Biochemistry*, *6*, 266 (1967).
(17) V. Marecĕk and J. Honz, *Collect. Czech. Chem. Commun.*, **38**, 965 (1973).
(18) W. T. Bresnahan, J. Moiroux, Z. Samec, and P. J. Elving, *Bioelectrochem. Bioenerg.*, 7, 125 (1980).

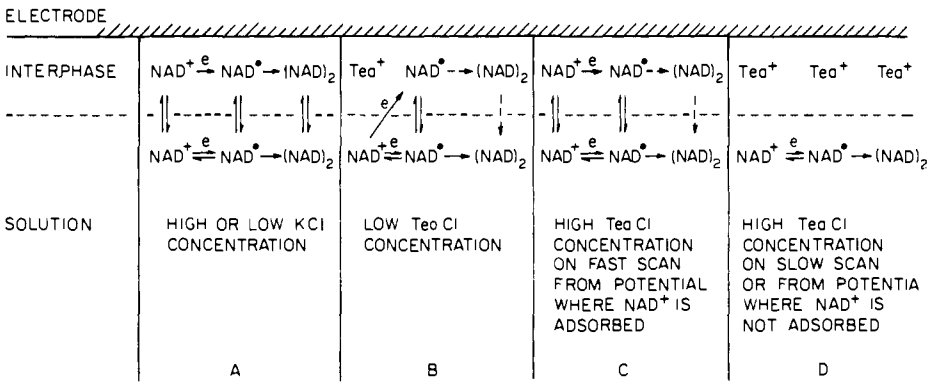

Figure 11. Mechanistic pathways for the initial one-electron reduction of NAD^+ under various conditions: A, 62.5 mM and 0.4 M KCl solutions; B, 62.5 mM and 0.1 M TeaCl solutions; C, 0.4 M TeaCl solution where NAD^+ is adsorbed; D, 0.4 M TeaCl solution with slow potential scan from a potential where NAD^+ is adsorbed or any scan from a potential where NAD^+ is not adsorbed.

significantly because the initial 1-e reduction is not sensitive to pH above pH 5,[8,19] and Tris and carbonate are not measurably surface active in the present solutions.

The time scale of the experiment and the initial state of the electrode surface, which is controlled by the initial potential (E_i) of the experiment, are important factors in determining the reaction pathways, e.g., a rapid potential sweep from a potential where NAD^+ is adsorbed will produce currents controlled by adsorption; a sufficiently slow sweep from the same E_i will produce a diffusion-controlled reduction when NAD^+ is desorbed at a potential positive of its reduction.

(1) In Absence of Surfactant. NAD^+ undergoes both diffusion- and adsorption-controlled reduction in KCl solutions (Figure 11A). Diffusion-controlled currents are observed on slow time scale experiments such as dc polarography and slow-scan CV; adsorption control predominates on the time scale of fast-scan CV. The absence of pre- or postprocesses indicates nearly equal strengths of adsorption for NAD^+ and NAD·. $(NAD)_2$ is adsorbed and only desorbs at potentials negative of −1.20 and −1.32 V in 63 mM and 0.4 M KCl solutions, respectively. An arrow for the oxidation of adsorbed NAD· is not shown in Figure 11A because the shape of the anodic peak on fast-scan CV indicates that it is diffusion controlled. The present results agree with those previously reported for situations involving diffusion-controlled currents.[8,19]

(2) In Presence of Low Surfactant Concentrations. NAD^+ undergoes two 1-e reduction processes in 63 and 100 mM TeaCl solutions at both slow and fast time scales; one process involves reduction to soluble products of NAD^+ as it diffuses to the electrode and the other to products which are adsorbed at the interface (Figure 11B). The adsorption-controlled process, which is not immediately evident with dc polarography but is revealed with pulse and ac polarography and CV, appears as a preprocess to the diffusion-controlled process and must involve the adsorption of NAD·; $(NAD)_2$ is, at most, transiently adsorbed since there is no ac quadrature peak for its desorption as is seen in KCl solution. Since only one anodic peak for NAD· oxidation is seen on fast-scan CV whose shape indicates diffusion control, single- and double-headed arrows are used for the adsorption-controlled preprocesses and the diffusion-controlled process, respectively. Since it is uncertain whether NAD· dimerizes in the interphase or in solution, the dashed arrows indicate that dimerization in the interphase would be followed by rapid desorption.

Tris is in no way responsible for the adsorption-controlled preprocess because the latter is not observed in the Tris–KCl solution and has been observed for 0.40 mM NAD^+ in 50 mM TeaCl and 50 mM carbonate (pH 9.0).[20]

(3) In Presence of High Surfactant Concentration. In CV experiments at high scan rate (v), two processes are observed for the NAD^+ reduction when E_i is −0.10 V, at which potential NAD^+ is adsorbed (Figure 11C). NAD^+ can be reduced under both adsorption and diffusion control as is evident from the variation of CV i_p with v; the adsorption-controlled process differs from that in 63 mM TeaCl (Figure 11B) in that no preprocess is observed. Therefore, the process is 0.4 M TeaCl, as in KCl, must involve adsorption of both NAD^+ and NAD·; i.e., NAD· is not more strongly adsorbed than NAD^+ under these conditions. On the basis of competition with Tea^+ for adsorption sites, NAD· is probably more weakly adsorbed from 0.4 M TeaCl than from 63 mM TeaCl. An arrow for oxidation of adsorbed NAD· is not shown in Figure 11C since the shape of the anodic peak indicates that it is diffusion controlled. The adsorption of $(NAD)_2$ is at most transient, since no ac tensammetric peak for it appears.

At low v with any E_i and at high v with an E_i of −0.9 V, where NAD^+ is not adsorbed, only the diffusion-controlled reduction of NAD^+ is observed (Figure 11D); i.e., a single peak appears, whose i_p is proportional to $v^{1/2}$ and whose shape is indicative of a diffusion-controlled process. Only under these conditions is it possible to determine the rate constant for the dimerization by using the current-ratio (i_{pa}/i_{pc}) method;[10] dimerization rate constants evaluated in the presence of adsorption may be erroneously high since i_{pa}/i_{pc} would be low. Furthermore, only under diffusion control is it possible to measure a meaningful heterogeneous rate constant for the 1-e reduction from CV data.

Acknowledgment. The authors thank the National Science Foundation which helped support the work described.

(19) C. O. Schmakel, Ph.D. Thesis, University of Michigan, Ann Arbor, 1971.

(20) J. Moiroux and P. J. Elving, unpublished results.